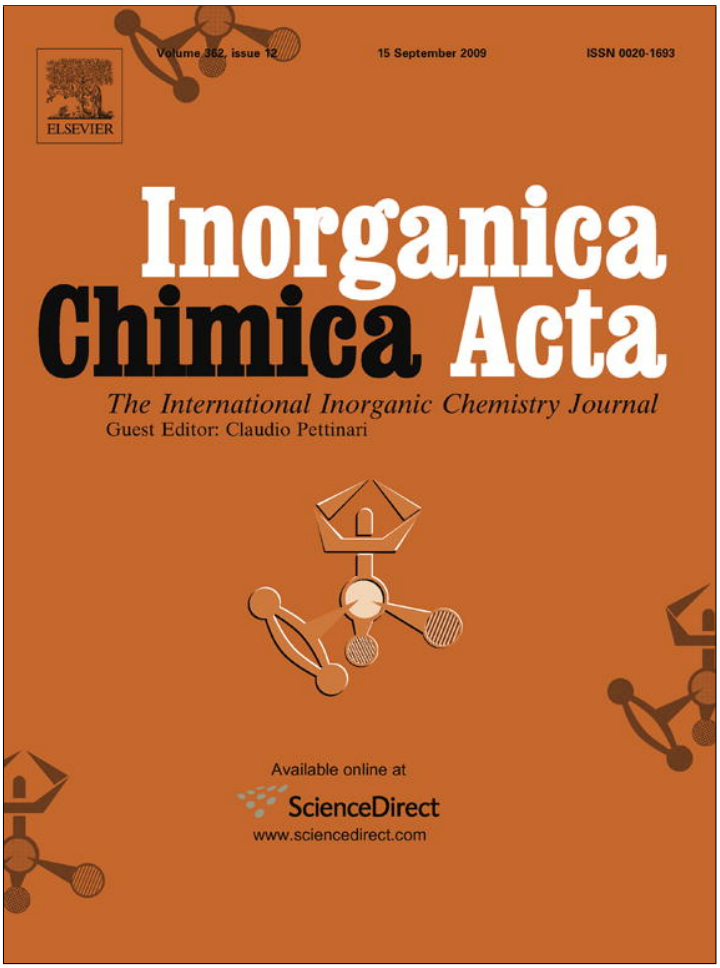

Inorganica Chimica Acta 362 (2009) 4340–4346

Contents lists available at ScienceDirect

Inorganica Chimica Acta

journal homepage: www.elsevier.com/locate/ica

Metalorganic frameworks based on the 1,4-bis(5-tetrazolyl) benzene ligand: The Ag and Cu derivatives

Angelo Maspero [a,*], Simona Galli [a,*], Valentina Colombo [a], Giulia Peli [a], Norberto Masciocchi [a], Stefano Stagni [b], Elisa Barea [c], Jorge A.R. Navarro [c]

[a] Dipartimento di Scienze Chimiche e Ambientali, Università dell'Insubria, via Valleggio 11, 22100 Como, Italy
[b] Dipartimento di Chimica Fisica ed Inorganica, Università di Bologna, viale Risorgimento 4, 40136 Bologna, Italy
[c] Departamento de Química Inorgánica, Universidad de Granada, Av. Fuentenueva S/N, 18071 Granada, Spain

ARTICLE INFO

Article history:
Received 22 July 2008
Accepted 29 November 2008
Available online 10 December 2008

Dedicated to the memory of Swiatoslaw (Jerry) Trofimenko

Keywords:
Metal organic frameworks
Nitrogen ligands
X-ray powder diffraction
Tetrazolate

ABSTRACT

The recently proposed high-yield synthesis of the 1,4-bis(5-tetrazolyl)benzene ligand (H_2btb) allowed the preparation of three new metal organic frameworks, namely Ag_2(btb), **1**, Cu_2(btb), **2**, and $Cu_2(OH)_2$(btb), **3**. These polycrystalline materials were fully characterised by spectroscopic, gas adsorption, thermal and diffraction methods, the latter revealing rather dense frameworks for **1** and **3**. Despite many different synthetic approaches, **2** invariably gave a poorly resolved, but highly reproducible, powder diffraction trace, hampering a complete structural characterisation. Magnetic measurements performed on **3** showed that it behaves as an antiferromagnetic material, the r.t. magnetic moment per Cu atom being only 1.24μ_B. The reactivity of **1** was proved in excess of triphenylphosphine (PPh_3), allowing the isolation of the dinuclear species **4**, $[(PPh_3)_3Ag]_2$(btb). An additional species **5**, formulated as $[(PPh_3)Ag]_2$(btb), could be selectively isolated on varying the reaction conditions; at variance, pyrazine, in solution or in molten form, did not react with **1**.

1. Introduction

In the last decade we have been deeply exploring the coordination chemistry of polydentate ligands possessing multiple donor sites. Originally, we employed simple heteroaromatic anions, such as pyrazolate [1], imidazolate [2] and pyrimidinolate [3]. Only at a later stage, we increased the complexity of the polytopic N-ligands, aiming at the formation of oligomeric and polymeric species with different functional properties. For example, using substituted triazines [4], bisimidazolates [5] and other substituted heterocycles [6], we have isolated and fully characterised several highly functional materials, such as catalytically active species (soluble oligomers [7] and insoluble 3D polymers [8]) or extended solids capable of molecular sensing and recognition [3,9]. Since many of these materials do not afford single crystals of suitable quality, we attained their full structural characterisation resorting to state-of-the-art powder diffraction methods, occasionally coupled to thermodiffractometry [10] and ^{13}C CP-MAS NMR spectroscopy [11].

Planning to employ polytopic longer spacers, concomitantly possessing increased coordination possibilities, we turned our attention to the 1,4-bis(5-tetrazolyl)benzene species ($C_8H_6N_8$, H_2btb, see Scheme 1), originally synthesised by Finnegan et al. [12], one of the most interesting ligands recently appeared in the literature.

A few papers dealing with the coordination properties of its deprotonated counterpart ($C_8H_4N_8$, btb) demonstrated its pronounced tendency in bridging distant metal ions [13] and in generating highly porous species, leading to efficient gas sensing, recognition and storage properties [14].

After having tailored high-yield, cheap and atoxic syntheses for H_2btb and for the analogous 1,4-bis(4-pyrazolyl)benzene species ($C_{12}H_{10}N_4$, H_2bpb) [15], we started coupling these ligands with a number of transition metal ions, aiming at the formation of microcrystalline materials of well defined stoichiometry, structure and functional properties: nanoporosity, cooperative magnetism and catalytic activity.

Therefore, in the following, our latest results on the silver and copper derivatives of btb will be presented, highlighting the dense packings of Ag_2(btb), **1**, and $Cu_2(OH)_2$(btb), **3**. In the absence of a proper structural model, a coherent picture of the nature of Cu_2(btb), **2**, is also traced, based on the analytical, thermal, spectroscopic and gas adsorption properties. These results follow a very recent report by Long and co-workers [16], who sagaciously employed bpb in the construction of a porous pseudotetragonal network, Co(bpb), stabilized by ancillary DMF ligands and clathrated solvent molecules.

* Corresponding authors.
E-mail address: simona.galli@uninsubria.it (S. Galli).

0020-1693/$ - see front matter © 2008 Elsevier B.V. All rights reserved.
doi:10.1016/j.ica.2008.11.031

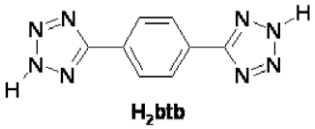

Scheme 1. Schematic drawing of the H_2btb species (the 2H tautomer is arbitrarily shown here).

2. Experimental

2.1. Materials and methods

Metal salts were used as received (Aldrich). H_2btb was prepared as described in Ref. [15]. Solvents were dried and distilled by standard methods. All preparations and manipulations were carried out under dinitrogen atmosphere using conventional Schlenk's techniques. Infrared spectra were recorded on a Shimadzu Prestige-21 instrument. Elemental analyses were carried out on a Perkin Elmer CHN Analyzer 2400 Series II. Simultaneous TG and DSC analyses were performed in a N_2 stream on a Netzsch STA 409 PC Luxx (heating rate: 10 °C min^{-1}). Magnetic measurements were performed on polycrystalline samples on a SQUID Quantum Design MPMS XL-5 in the 2–300 K temperature range applying external fields of 10 000 Oe. Adsorption isotherms of Ar and N_2 were measured at 77 K on a Micromeritics Tristar 3000 volumetric instrument. Prior to measurement, powder samples were heated at 373 K for 12 h and outgassed to 10^{-6} Torr using a Micromeritics Flowprep.

2.2. Synthesis of Ag_2(btb) (**1**)

To a solution of $AgNO_3$ (0.159 g, 0.94 mmol) in water (6 mL), solid H_2btb (0.100 g, 0.48 mmol) was added in one single portion. The reaction was refluxed for 5 h under stirring. After the mixture was cooled at room temperature, the white precipitate was filtered off, washed with water and dried in vacuum at room temperature to afford the desired product **1**. IR(nujol): ν = 845 and 741 cm^{-1} (C–H bending of btb). *Anal.* Calc. for $C_8H_4Ag_2N_8$ (427.7 g mol^{-1}): C, 22.44; H, 0.94; N, 26.18%. Found: C, 23.36; H, 1.16, N, 25.68%.

2.3. Synthesis of Cu_2(btb) (**2**)

To a suspension of 1,4-bis(5-tetrazolyl)benzene (0.100 g, 0.47 mmol) in acetonitrile (4 mL) triethylamine (1.0 mL) was added, under dinitrogen atmosphere and at room temperature; after warming the mixture to 70 °C, it was kept under stirring until a yellow solution formed. To this solution, an acetonitrile solution (2 mL) of $[Cu(CH_3CN)_4]BF_4$ (0.293 g, 0.93 mmol) was then added dropwise. A white suspension formed, which was then refluxed for 4 h. The precipitate was filtered, washed with acetonitrile and dried in vacuum to afford the desired product **2**. *Anal.* Calc. for $C_8H_4Cu_2N_8$ (339.3 g mol^{-1}): C, 28.15; H, 1.17; N, 32.8%. Found: C, 28.90; H, 1.80, N, 31.79%.

2.4. Synthesis of $Cu_2(OH)_2$(btb) (**3**)

To a suspension of $Cu(ClO_4)_2$ $6H_2O$ (0.173 g, 0.47 mmol) in 1-butanol (6 mL), 1,4-bis(5-tetrazolyl)benzene (0.060 g, 0.28 mmol) was added, at room temperature, under stirring. The mixture was heated to 95 °C and kept at this temperature for 15 min. Triethylamine (1.0 mL) was subsequently added to the mixture. The reaction was then kept at 95 °C for 4 h. The blue precipitate was filtered off, washed with methanol and dried in vacuum. IR(nujol): ν = 3551 cm^{-1} (O–H stretching), 852 and 742 cm^{-1} (C–H bending of btb). *Anal.* Calc. for $C_8H_6Cu_2N_8O_2$ (373.3 g mol^{-1}): C, 25.74; H, 1.60; N, 30.02%. Found: C, 28.36; H, 2.09, N, 29.16%.

2.5. Preparation of $[(PPh_3)_3Ag]_2$(btb) (**4**)

To a suspension of triphenylphosphine (0.980 g, 3.74 mmol) and 1,4-bis(5-tetrazolyl)benzene (0.100 g, 0.47 mmol) in acetonitrile, triethylamine (1.0 mL) was added in one single portion. The suspension was stirred at room temperature until a yellow solution formed. To this solution, $AgNO_3$ (0.159 g, 0.94 mmol) was added and the suspension was kept at 70 °C under stirring for 4 h. The white product was filtered off, washed with acetonitrile and diethyl ether and dried in vacuum. IR(nujol): ν = 748 cm^{-1} (C–H bending of btb), 743 and 696 cm^{-1} (C–H bending of PPh_3). *Anal.* Calc. for $C_{120}H_{100}Ag_2N_{10}P_6$ (2083.8 g mol^{-1}): C, 69.17; H, 4.84; N, 6.72%. Found: C, 68.84; H, 4.85, N, 6.86%. Colorless single crystals suitable for conventional X-ray diffraction analysis were obtained by slow diffusion of a solution of H_2btb, PPh_3 and Et_3N into a solution of $AgNO_3$ in acetonitrile.

2.6. Preparation of $[(PPh_3)Ag]_2$(btb) (**5**)

To a suspension of **1** (0.100 g, 0.234 mmol) in acetonitrile, triphenylphosphine (0.153 g, 0.584 mmol) was added at room temperature in one portion (Ag:PPh_3 ratio of 1:2.5). The white suspension was then kept overnight under stirring. The white derivative was filtered off, washed with acetonitrile, diethyl ether and dried under vacuum. IR(nujol): ν = 743 and 696 cm^{-1} (C–H bending of PPh_3). *Anal.* Calc. for $C_{44}H_{34}Ag_2N_8P_2$ (952.50 g mol^{-1}): C, 55.48; H, 3.60; N, 11.76%. Found: C, 55.88; H, 3.77, N, 10.48%.

2.7. X-ray powder diffraction analysis

Powdered, microcrystalline samples of **1, 2** and **3** were gently ground in an agate mortar, then deposited in the hollow of an aluminium sample holder (equipped with a zero-background plate). The data were collected with overnight scans in the 5–105° 2θ range on a Bruker AXS D8 Advance diffractometer, equipped with a linear position-sensitive Lynxeye detector, primary beam Soller slits, and Ni-filtered Cu Kα radiation (λ = 1.5418 Å). Generator setting: 40 kV, 40 mA. Standard peak search, followed by indexing with TOPAS [17], allowed the detection of the approximate unit cell parameters: a = 19.83, b = 13.50, c = 7.00 Å, (GOF 62), for **1**, and a = 3.60, b = 5.99, c = 12.71 Å, α = 84.9, β = 96.2 and γ = 87.9°, (GOF 46), for **3**. Structure solutions were performed, in *Fddd* and $P\bar{1}$ (for **1** and **3**, respectively), with the simulated annealing technique, as implemented in TOPAS, using a rigid, idealised, molecular fragment of known D_{2h} geometry for btb, a metal ion and, where pertinent, an OH residue. For **3**, which shows anisotropically broadened peaks, only *approximate* atom locations could be derived, given that neither simple nor complex microstructural models, refinable in TOPAS, could match the observed profile intensity. A structural interpretation of this behaviour is provided below in the Section 3. The final refinements were carried out with the Rietveld method, maintaining the rigid body described above and allowing the refinement of the torsion angles of the heterocyclic rings linkage. The background was modelled by a polynomial function. One, refinable isotropic thermal parameter was assigned to the metal atoms, augmented by 2.0 $Å^2$ for lighter atoms. A preferred orientation correction was introduced (in the March–Dollase formulation) along the [1 0 0] and [0 0 1] directions for **1** and **3**, respectively. Final Rietveld refinement plots are shown in Fig. 1.

Crystal data for ***1****:* $C_8H_4Ag_2N_8$, *fw* = 427.7 g mol^{-1}; orthorhombic, *Fddd*, a = 19.8216(6), b = 13.4975(4), c = 6.9836(3) Å; V = 1868.4 (1) $Å^3$; Z = 8; ρ_{calc} = 3.040 g cm^{-3}; F(0 0 0) = 1616; μ(Cu Kα) =

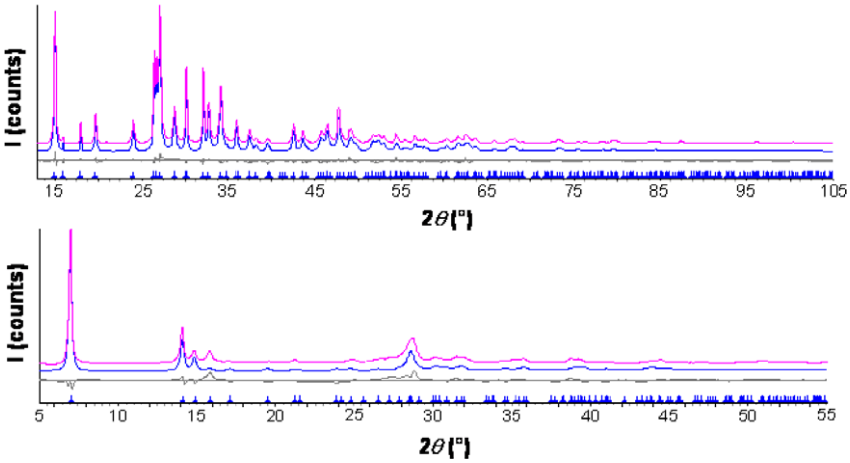

Fig. 1. Rietveld refinement plots for Ag_2(bpb) **1** (top) and $Cu_2(OH)_2$(bpb) **3** (bottom) with peak markers and difference plot at the bottom. Top trace: observed data. Horizontal axis: 2θ, deg; vertical axis: counts.

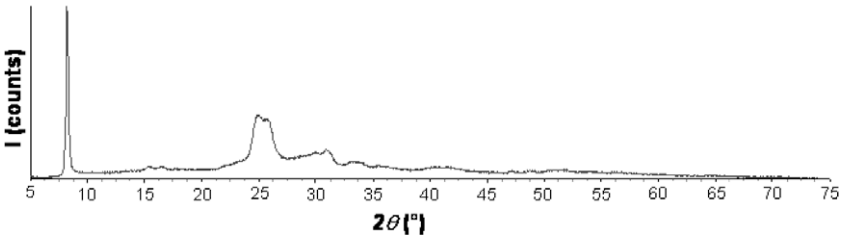

Fig. 2. Raw diffraction data for Cu_2(bpb) **2**. Horizontal axis: 2θ, deg; vertical axis: counts.

337.4 cm^{-1}. R_p, R_{wp} and R_{Bragg}, 0.030, 0.040, and 0.015, respectively, for 31 parameters [18].

Crystal data for ***3****:* $C_8H_6Cu_2N_8O_2$, *fw* = 373.3 g mol^{-1}; triclinic, $P\bar{1}$, a = 3.743(2) Å, b = 5.980(5) Å, c = 12.668(5) Å; α = 84.48(5)°; β = 95.80(6)°; γ = 89.01(6)°; V = 280.7(2) $Å^3$; Z = 1; ρ_{calc} = 2.208 g cm^{-3}; $F(000)$ = 368; μ(Cu Kα) = 48.7 cm^{-1}. R_p, R_{wp} and R_{Bragg}, 0.075, 0.103, and 0.061, respectively [19].

Unfortunately, the highly reproducible powder diffraction trace of pure **2** (shown in Fig. 2), speaks for a very defective phase, where the extreme broadening (tanθ dependent?) of the diffraction peaks can be easily interpreted by a heavily strained structure, lacking long order periodicity. Work can be anticipated in obtaining a more crystalline phase, allowing to elucidate the structure of **2**.

2.8. Thermodiffractometry

On the basis of the results of the simultaneous thermal analysis, the thermal behaviour of species **3** was further investigated by employing a custom-made sample heater (supplied by Officina Elettrotecnica di Tenno, Italy), mounted on the Bruker AXS Advance D8 diffractometer. A powdered, microcrystalline batch of **3** was manually ground in an agate mortar, then deposited in the hollow of an aluminium sample-holder. A sequence of scans, in the 5–22° 2θ range, was performed heating *in situ* from room temperature up to 330 °C.

2.9. Single-crystal diffraction analysis

The X-ray diffraction data from a prismatic crystal of **4** · **2CH_3CN**, mounted on the top of a glass fibre of a goniometer head, were measured at room temperature by means of a Nonius CAD4 diffractometer using Mo Kα radiation (λ = 0.71073 Å). Local programs were used for cell refinement and data reduction. An empirical absorption correction was applied to all of the data (psi-scan). The structure was solved by direct methods using SHELXS-97 [20], with the WINGX graphical user interface [21]. Structural refinement was carried out using SHELXL-97. All non-H atoms were refined anisotropically, whilst aromatic hydrogen atoms were constrained to ride on their parent atom with U_{iso} = 1.2 U_{eq} (parent atom). No H atoms were included in the clathrated CH_3CN molecule, the geometry of which was restrained to reference values.

Crystal data for ***4*** · ***2CH₃CN****:* $C_{120}H_{100}Ag_2N_{10}P_6$, *fw* = 2083.8 g mol^{-1}; triclinic, $P\bar{1}$, a = 13.506(6), b = 13.939(4), c = 14.052(7) Å, α = 83.45(3), β = 78.90(3), γ = 87.44(4)°; V = 2679(2) $Å^3$, Z = 1; ρ_{calc} = 1.342 g cm^{-3}; $F(000)$ = 1074; μ(Mo Kα) = 5.28 cm^{-1}. R and $wR2$, 0.067 and 0.172, for 7349 observed data and 630 refined parameters.

3. Results and discussion

3.1. Synthetic and analytical aspects

The reaction of $AgNO_3$ with H_2btb in water at 120 °C, in the absence of added bases, affords a white product which, on the basis of elemental analysis and IR data was formulated as Ag_2(btb), **1**. Indeed, the infrared spectrum of **1** recorded in the solid state (nujol) shows two sharp absorptions at 845 and 741 cm^{-1}, attributed to the bending of the aromatic C–H of the btb ligand, whilst no N–H, nor hydrogen bonded N–H···N IR fingerprints were observed.

The polymeric nature of species **1** was initially suggested by its extreme insolubility in most solvents and then confirmed by the XRPD study (see below). Compound **1** is chemically very inert: in fact, no reaction is observed between this species and nitrogen-containing Lewis bases, such as pyrazine, even on adopting a variety of reaction conditions. However, employing a P-based ligand

such as triphenylphosphine (with an Ag:PPh_3 ratio of 1:2.5) a new derivative was isolated, $[(PPh_3)Ag]_2$(btb), **5**, the formulation of which was suggested by elemental analysis and IR data. Accordingly, the infrared spectrum of **5**, recorded in the solid state (nujol), shows two sharp bands at 743 and 696 cm^{-1}, which are assigned to the bending of the aromatic C–H of PPh_3.

The poor solubility of **5**, hampering the preparation of suitable single crystals, and its structural complexity (beyond the present possibility of a meaningful powder diffraction characterisation), did not allow the determination of the correct connectivity and its complete geometrical formulation.

Differently, if an acetonitrile solution of $AgNO_3$ is added dropwise, at room temperature, to an acetonitrile solution containing H_2btb, PPh_3 and Et_3N, a different complex is obtained, $[(PPh_3)_3Ag]_2$(btb) (**4**). The IR spectrum of **4**, recorded in the solid state (nujol), shows, beside the bending of the aromatic C–H of the azolate ligand at 748 cm^{-1}, two extra absorptions at 743 and 696 cm^{-1}, assigned to the bending of the C–H fragments of triphenylphosphine. The dinuclear nature of species **4** was later confirmed by single-crystal X-ray diffraction analysis.

If $[Cu(CH_3CN)_4]BF_4$ is reacted with H_2btb in acetonitrile at room temperature, in presence of triethylamine), species **2** can be easily isolated as an analytically pure, white, air stable product, of Cu_2(btb) stoichiometry.

Cu(II) salts were also employed: on reacting $Cu(ClO_4)_2 \cdot 6H_2O$ with H_2btb in 1-butanol, at 95 °C and in presence of triethylamine, a blue product of $Cu_2(OH)_2$(btb) formulation, **3**, can be isolated. The IR spectrum of **3**, recorded in the solid state (nujol), shows a sharp absorption at 3551 cm^{-1}, attributed to the stretching of the O–H group (not involved in hydrogen bond interactions), as well as two sharp bands at 852 and 742 cm^{-1} (bending of the aromatic C–H of the btb ligand).

Aiming at the preparation of the elusive [14] homoleptic Cu(btb) complex, the same reaction was carried out at 120 °C, a new species being isolated as a light brown product. As demonstrated by the equivalence of the XRPD trace of this beige product with that of **2** (shown above), this material is essentially a mixture of the copper(I) polymer, Cu_2(btb), **2**, and of a minor Cu(II) impurity (possibly CuO), not detected in the XRPD trace [22]. Despite the different reaction conditions employed in the preparation of Cu(II) complexes in rigorously anhydrous conditions, the reducing capabilities of 1-butanol at high temperature always generated the rather stable, but poorly crystalline, Cu_2(btb) species.

3.2. Thermoanalytical results

We have also investigated the thermal behaviour of **1**, **2** and **3** by simultaneous (TG and DSC) thermal analyses. Interestingly, **1** is stable up to 380 °C, where a sudden decomposition starts, accompanied by a very large exothermic peak (ΔH = −133 kJ mol^{-1}). This behaviour is attributed to the oxidising character of the Ag(I) ions, capable of eliminating simple gaseous molecules (N_2, HCN, etc.) from the heterocyclic rings.

At variance, **2** showed *ca.* 8% weight loss below 250 °C, likely attributed to solvent molecules, trapped in the *small* pores of the structure (*vide infra*). After this smooth release, complete decomposition of the material occurs above 350 °C, with a large enthalpy release (ΔH = −61.0 kJ mol^{-1}). What is here relevant are the rather high decomposition temperatures observed for **1** and **2**, particularly after considering that tetrazoles are widely employed in commercial explosives and detonators [23].

Finally, **3** was found to decompose above 270 °C in a two-step process, the first peaking at about 300 °C and the second near 330 °C (ΔH_{TOT} = −113 kJ mol^{-1}). The thermodiffractometric measurements performed *in situ* in the diffractometer chamber could not discriminate between the two, partial superimposed steps, decomposition above 300 °C being the only detectable event. Thus, no definitive analytical or structural information on the intermediate species could be derived. Notably, the first jump in the TG experiments accounts for a 17.85% weight loss (33.3 amu), nicely matching the loss of two hydroxyls, in an internal redox reaction as in:

$$Cu_2(OH)_2(btb) \rightarrow Cu_2(btb) + H_2O + 1/2O_2. \quad (1)$$

Indeed, formation of Cu(I) azolates from high temperature treatment of Cu(II) precursors has already been observed [24].

3.3. Structural characterisation of *1*, *2* and *3*

Our XRPD structure determination of **1** revealed the existence of a complex, dense network based on btb ligands (lying on a 222 symmetry site), connected through all their eight N atoms to eight different, but crystallographically equivalent, Ag ions (each one sitting on a twofold axis aligned with **a**). Fig. 3 shows a portion of this complex packing, in which a sequence of condensed hexanuclear –Ag–N–N–Ag–N–N– rings zigzags in the **a** + **c** direction, with Ag···Ag contacts of 3.92 Å. Further contacts of 3.98 Å interconnect these 1D strands, giving to the silver ion sublattice an overall 3 D topology. Two (crystallographically unique) Ag–N–N–Ag torsion angles are present: Ag–N1–N2–Ag (43.9°, indicating a skew conformation for such tetraazadimetallacycle) and 18.5° for Ag–N1–N1–Ag (generating a more planar ring) [numbering scheme from the supplied CIF files]. Finally, the refined torsion angle between the tetrazolate and benzene rings, of about 8.7(2)°, speaks for a nearly planar system for the three conjugated aromatic rings, maintaining extensive π–π overlap.

Compound **3** crystallizes in the triclinic $P\bar{1}$ space group, with one independent Cu(II) ion, one btb ligand lying about **a** −1position, and bridging four crystallographically equivalent metal ions along **b**, and one μ_3-OH ligand, bridging three crystallographically equivalent metal centres. Fig. 4 shows a portion of the complex packing: hexanuclear –Cu–N–N–Cu–N–N– rings are bridged by OH groups in the **b** direction. On viewing down [001], parallel ladders of Cu(OH) formulation, running along **a**, can be easily

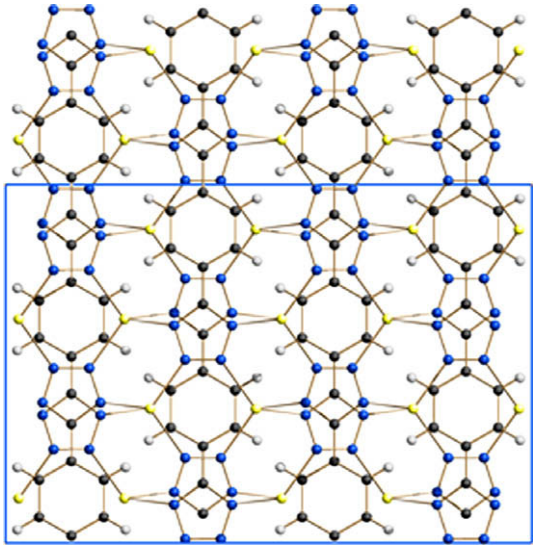

Fig. 3. Schematic drawing of the structure of Ag_2(btb) **1**, viewed down [001], as derived by our powder diffraction analysis. Cell edges are drawn as solid lines. Given the complexity of this dense packing, the interested reader is invited to download the pertinent CIF file from the Electronic Supplementary Information for a clearer 3D structure visualisation. Relevant geometrical parameters: shortest Ag···Ag 3.92 and 3.98 Å, Ag–N1 2.47(3), Ag–N2 2.27(6) Å, tetrazole–benzene torsion angle 8.7(2)°.

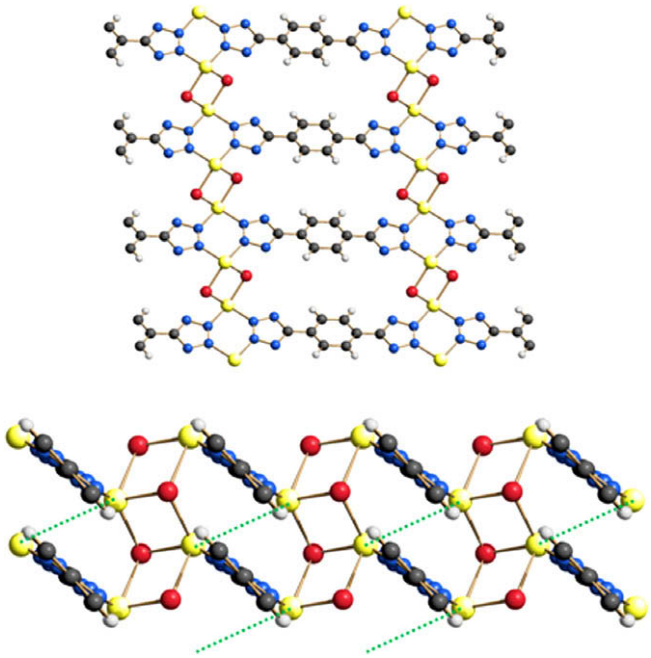

Fig. 4. Schematic drawing of structure of $Cu_2(OH)_2(btb)$ **3**, as derived by our powder diffraction analysis; top, viewed down [100], bottom, down [001].

envisaged, mutually linked by the most "external" nitrogen atoms which bind Cu(II) ions as normally pyrazolates do.

The green dashed lines in Fig. 4 indicate the alternative locations that the nearly parallel btb ligands may adopt: if no, or little, influence amongst neighbouring columns of π–π stacked btb ligands (separated by the **a** axis distance of about 3.74 Å) is present, one expects a nearly random disorder (which we tried to model during data analysis, without significant success). In the case of a conditioned disorder, with a "reversing" probability significantly different from 0 (a perfect crystal) or 0.5 (random disorder), a highly defective material is generated, with the obvious consequence of evident, but poorly treatable, peak broadening. Accordingly, the structure of **3** is not discussed here in detail, but only presented in a semiquantitative manner. Worthy of note, a closely related system, $Co(OH)_2$(benzene-1,4-dicarboxylate), also showed a significant disorder of the organic ligand stackings; yet, in that case, the absence of cross-talking between adjacent stacks was easily detected, and interpreted, by the experimental rise of space group symmetry [25].

As anticipated, our XRPD data could not be used in unravelling the structural model for **2** (a highly defective phase, see above); however, and rather surprisingly, the *d*-spacing of the strongest, and sharpest, peak (10.8 Å) is not consistent with the Cu···Cu distance expected for a stretched polymer, in which the btb fragments bridge Cu(I) ions with their "external" nitrogen atoms. Also, **1** and **2**, despite sharing the same stoichiometry, are not isomorphous species.

Therefore, the apparently simple (local) structure might be somewhat different, perhaps based on trinuclear moieties (ubiquitous in Cu(I) azolates [26]), packed in porous hexagonal sheets. In order to gain some external, independent, information in this respect, we have measured the adsorptive properties of **2** towards N_2 and Ar (at 77 K).

3.4. Gas sorption properties of *2*

The adsorption isotherm of **2** towards N_2 (Fig. 5) possesses a type I–IV hybrid shape, with a (type H1) hysteresis loop at relative

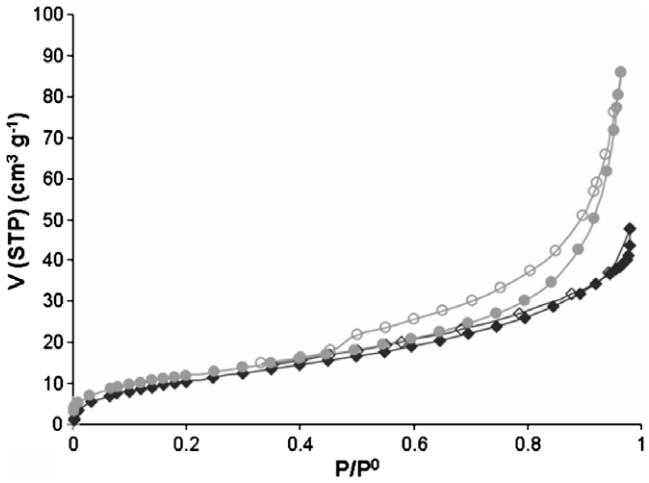

Fig. 5. N_2 (red) and Ar (blue) adsorption isotherms at 77 K for Cu_2(btb), **2**. Full and open symbols denote adsorption and desorption, respectively. (For interpretation of the references to colour in this figure legend, the reader is referred to the web version of this article.)

pressures (above $p/p_0 = 0.4$), which can be attributed to textural mesoporosity arising from interparticle mesopores. Our results show that **2** possesses Langmuir surface areas of 60 and 50 $m^2\ g^{-1}$, as calculated from the N_2 and Ar adsorption isotherms, respectively. The moderate Langmuir surface area and gas-storage capacity for both gases are likely related to a poor diffusion of these gaseous molecules, possibly linked to a partial sliding of the (weakly interacting) layers on top of each other, giving rise to an offset packing with small channel dimensions. This kind of behaviour is typical of layered porous networks and therefore it supports this probable structural model [27].

3.5. Crystal structure of complex *4* · *2CH₃CN*

Species **4** · **2CH₃CN** crystallizes in the triclinic space group $P\bar{1}$. It contains dinuclear complexes of $[(PPh_3)_3Ag]_2$(btb) formulation (Fig. 6), co-crystallized with acetonitrile solvent molecules, and in which the btb molecule bridges the two Ag(I) ions (13.36 Å apart). The coordination mode of this ligand deserves a few comments: (i) despite its polydentate nature, with up to eight N donor sites, only two (one on each heterocyclic ring) are directly bound to the metal ions [Ag–N 2.347(4) Å], and (ii) Ag(I) ions lie well below the least-squares plane of the tetrazolate residue (by about 1.35 Å),

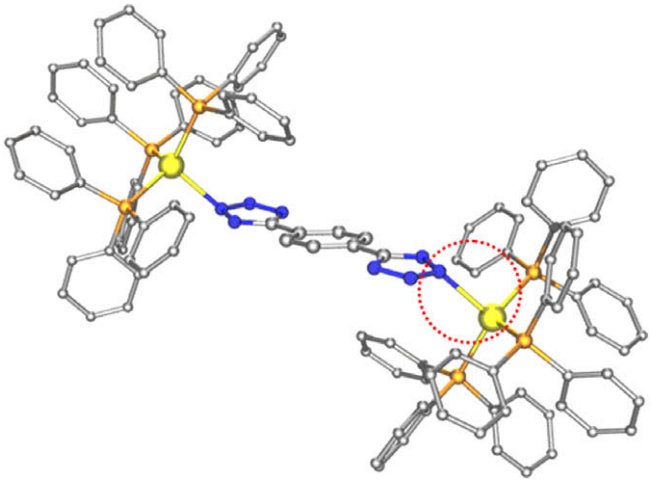

Fig. 6. Schematic drawing of the molecular structure of $[(PPh_3)_3Ag]_2$(btb), **4**, highlighting the unusual off-plane Ag–N bond, discussed in the text.

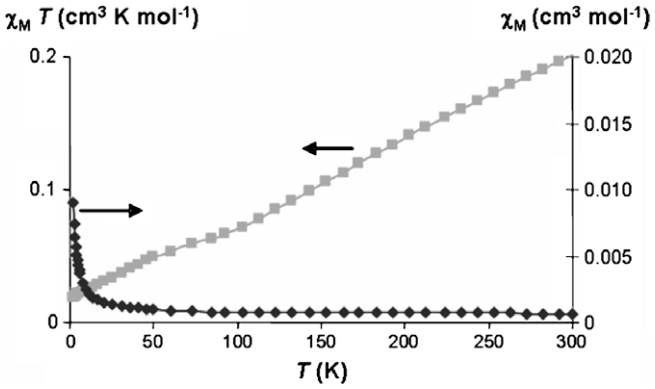

Fig. 7. Thermal dependence of the magnetic susceptibility for $Cu_2(OH)_2$(btb), **3**.

as also witnessed by a N3–N2–N1–Ag torsion angle (137.6°) significantly different from 180°.

In **4**, as in **1**, the twist of the tetrazolate–benzene link is low (9.9°), suggesting a nearly optimised conjugated system. These observations speak for a rather high flexibility of the btb-Ag linkage, which, depending on the presence, or absence (as in **1**), of ancillary ligands (three bulky PPh_3 groups in **4**), may adapt itself in a variety of conformations.

*3.6. Magnetic properties of **3***

The thermal behaviour of the magnetic susceptibility for **3** is shown in Fig. 7. The data agree with a strong antiferromagnetic exchange between the copper(II) centres [28]. This is manifested by the low value at r.t. with a magnetic moment per Cu atom of only $1.24\mu_B$, which steadily decreases to $0.38\mu_B$ at 2 K. Unfortunately, the 3D nature of the network and the complex connectivity of the copper(II) ions, which are connected by btb and hydroxide bridges, preclude the finding of a suitable fitting model.

4. Conclusions

Summarizing, we have here presented the synthesis, characterisation and powder diffraction studies of novel polymeric group 11 metal complexes. The isolated materials are either dense or moderately porous and, therefore, they are not prone to gas sorption or storage, as originally targeted. Nevertheless, the btb ligand they contain shows a high chemical and thermal inertness, suggesting that suitably organised porous frameworks might possess relevant stability.

Work can be anticipated in the direction of preparing metal complexes with different metal ions and stoichiometry, as well as by tailoring new syntheses of related polyazolates, capable of linking metal centres with different topological features.

Worthy of note, the structures presented in this contribution have been derived from powder diffraction data of less-than-ideal polycrystalline materials. In these cases, laboratory data well compare with state-of-the-art synchrotron ones, since the instrumental resolution functions are well hidden in the large (anisotropic) peak broadening stemming from the sample microstructure.

Acknowledgements

This work was supported by MUR (PRIN2006: "Materiali Ibridi Metallo-Organici Multifunzionali con Leganti Poliazotati" and Azione Integrata Italia-Spagna) and Fondazione CARIPLO (Project No. 2007-5117). E.B. thanks the University of Granada for a "Contrato de Incorporación de Doctores".

Appendix A. Supplementary material

CCDC 695477, 695477, 695479 contain the supplementary crystallographic data for compounds **1**, **3** and **4**, respectively. These data can be obtained free of charge from The Cambridge Crystallographic Data Centre via www.ccdc.cam.ac.uk/data_request/cif. Supplementary data associated with this article can be found, in the online version, at doi:10.1016/j.ica.2008.11.031.

References

[1] A. Cingolani, S. Galli, N. Masciocchi, L. Pandolfo, C. Pettinari, A. Sironi, J. Am. Chem. Soc. 227 (2006) 6144, and references therein.
[2] (a) N. Masciocchi, S. Bruni, E. Cariati, F. Cariati, S. Galli, A. Sironi, Inorg. Chem. 40 (2001) 5897;
(b) N. Masciocchi, G.A. Ardizzoia, S. Brenna, F. Castelli, A. Maspero, S. Galli, A. Sironi, Chem. Commun. (2003) 2018.
[3] J.A.R. Navarro, E. Barea, A. Rodriguez-Dieguez, J.M. Salas, C.O. Ania, J.B. Parra, N. Masciocchi, S. Galli, A. Sironi, J. Am. Chem. Soc. 230 (2008) 3978, and references therein.
[4] H. Casellas, O. Roubeau, S.J. Teat, N. Masciocchi, S. Galli, A. Sironi, P. Gamez, J. Reedijk, Inorg. Chem. 46 (2007) 4583.
[5] (a) N. Masciocchi, A. Figini Albisetti, A. Sironi, C. Pettinari, A. Marinelli, Powder Diffr. 22 (2007) 236;
(b) N. Masciocchi, C. Pettinari, E. Alberti, R. Pettinari, C. Di Nicola, A. Figini Albisetti, A. Sironi, Inorg. Chem. 46 (2007) 10491;
(c) N. Masciocchi, C. Pettinari, E. Alberti, R. Pettinari, C. Di Nicola, A. Figini Albisetti, A. Sironi, Inorg. Chem. 46 (2007) 10501.
[6] (a) E. Barea, M.A. Romero, J.A.R. Navarro, J.M. Salas, N. Masciocchi, S. Galli, A. Sironi, Inorg. Chem. 44 (2005) 1472;
(b) S. Galli, N. Masciocchi, E. Cariati, A. Sironi, E. Barea, M.A. Haj, J.A.R. Navarro, J.M. Salas, Chem. Mater. 17 (2005) 4815;
(c) N. Masciocchi, S. Galli, A. Sironi, E. Cariati, M.A. Galindo, E. Barea, M.A. Romero, J.M. Salas, J.A.R. Navarro, F. Santoyo-Gonzalez, Inorg. Chem. 45 (2006) 7612.
[7] (a) G.A. Ardizzoia, M.A. Angaroni, G. La Monica, F. Cariati, S. Cenini, M. Moret, N. Masciocchi, Inorg. Chem. 30 (1991) 4347;
(b) G.A. Ardizzoia, S. Cenini, G. La Monica, N. Masciocchi, M. Moret, Inorg. Chem. 33 (1994) 1458.
[8] (a) F. Llabrés i Xamena, A. Abad, A. Corma, H. Garcia, J. Catal. 250 (2007) 294;
(b) F. Llabrés i Xamena, O. Casanova, R.G. Tailleur, H. Garcia, A. Corma, J. Catal. 255 (2008) 220.
[9] (a) J.A.R. Navarro, E. Barea, J.M. Salas, N. Masciocchi, S. Galli, A. Sironi, C.O. Ania, J.B. Parra, Inorg. Chem. 45 (2006) 2397;
(b) E. Barea, J.A.R. Navarro, J.M. Salas, N. Masciocchi, S. Galli, A. Sironi, J. Am. Chem. Soc. 126 (2004) 3014.
[10] S. Galli, N. Masciocchi, G. Tagliabue, A. Sironi, E. Barea, J.M. Salas, L. Mendez, M. Domingo, M. Perez-Mendoza, J.A.R. Navarro, Chem. Eur. J. 14 (2008) 9890.
[11] N. Masciocchi, S. Galli, E. Alberti, A. Sironi, C. Di Nicola, C. Pettinari, L. Pandolfo, Inorg. Chem. 45 (2006) 9064.
[12] W.A. Finnegan, R.A. Henry, R. Lofquist, J. Am. Chem. Soc. 80 (1958) 3908.
[13] S. Stagni, A. Palazzi, S. Zacchini, B. Ballarin, C. Bruno, M. Marcaccio, F. Paolucci, M. Monari, M. Carano, A.J. Bard, Inorg. Chem. 45 (2006) 695, and references therein.
[14] M. Dincă, A.F. You, J.R. Long, J. Am. Chem. Soc. 128 (2006) 8904.
[15] A. Maspero, S. Galli, N. Masciocchi, G. Palmisano, Chem. Lett. 37 (2008) 956.
[16] H.J. Choi, M. Dincă, J.R. Long, J. Am. Chem. Soc. 130 (2008) 7848.
[17] V. 3.0, Bruker AXS. Karlsruhe, Germany, 2005.
[18] The best profile and R_{Bragg} agreement factors were obtained upon freeing the Ag atom occupancy, which refined to 0.834(2). If this model is correct, some substitutional H/Ag disorder must be present, leading to a slightly different stoichiometry, i.e. $Ag_{1.66}H_{0.34}$(btb), without significant changes in the overall discussion. Indeed, protonation of the N1 or N2 sites (see the supplied CIF file for numbering) is geometrically compatible with the observed structural model, and might be responsible for the slight broadening of the diffraction peaks, which we attribute to compositional strain effects.
[19] As anticipated, no matter which synthetic procedure was adopted (changing temperature, solvent and reaction times), **3** systematically afforded powdered materials of rather poor crystallinity. Therefore, the quantitative assessment of the true lattice metrics and of the atomic coordinates in the unit cell cannot be reached. Nevertheless, the structural description reported above, as well as the overall nature, connectivity and topology of this 3D polymer are well defined. Since statistically significant values cannot be given, much care should be however taken in relying on the e.s.d.'s reported in this paper for the lattice parameters (and for the details of the structural model) of such a defective species.
[20] G.M. Sheldrick, Program for the Refinement of Crystal Structures, University of Göttingen, Germany, 1997.
[21] L.J. Farrugia, J. Appl. Cryst. 32 (1999) 837.
[22] Accordingly, our magnetic measurements indicated, for this material, a weak paramagnetic character (at rt), easily attributed to the Cu(II) impurity.
[23] F.R. Benson, Chem. Rev. 41 (1947) 1.

[24] M.K. Ehlert, S.J. Rettig, A. Storr, R.C. Thompson, J. Trotter, Can. J. Chem. 68 (1990) 1444.
[25] Z.-L. Huang, M. Drillon, N. Masciocchi, A. Sironi, J.-T. Zhao, P. Rabu, P. Panissod, Chem. Mater. 12 (2000) 2805.
[26] H.V.R. Dias, H.V.K. Diyabalanage, M.G. Eldabaja, O. Elbjeirami, M.A. Rawashdeh-Omary, M.A. Omary, J. Am. Chem. Soc. 127 (2005) 7489, and references therein.
[27] (a) E. Barea, M. Quirós, J.A.R. Navarro, J.M. Salas, Dalton Trans. (2005) 1743; (b) E. Barea, A. Rodríguez-Diéguez, J.A.R. Navarro, G. D'Alfonso, A. Sironi, Dalton Trans. (2008) 1825.
[28] A. Rodíguez-Diéguez, M.A. Palacios, A. Sironi, E. Colacio, Dalton Trans. (2008) 2887.